



ELSEVIER

Physica A 315 (2002) 203–214

PHYSICA A

www.elsevier.com/locate/physa

# Thermal fluctuations and their ordering in turbulent convection<sup>☆</sup>

J.J. Niemela<sup>a,\*</sup>, K.R. Sreenivasan<sup>b</sup>

<sup>a</sup>*Department of Physics, Cryogenic Helium Turbulence Laboratory, University of Oregon, Eugene, OR 97403, USA*

<sup>b</sup>*Institute for Physical Science and Technology, University of Maryland, MD 20742, USA*

---

## Abstract

In highly nonlinear thermal convection, random fluctuations within the flow organize themselves into a self-sustaining large-scale circulation. We experimentally study some properties of this mean “wind”, including the irregular reversal of its direction. We show that the energy in the organized motion is a small fraction of the thermal energy input, and becomes increasingly smaller as the Rayleigh number increases. A rough correspondence can be made to self-organized criticality from the analysis of various probability density functions associated with the fluctuating wind.

© 2002 Elsevier Science B.V. All rights reserved.

*PACS:* 67.40.Vs; 47.27.Gs; 47.37.+q

*Keywords:* Rayleigh number; Turbulent convection

---

## 1. Introduction

Thermal convection is an ubiquitous phenomenon that occurs on many scales and in many circumstances, from the drying of a thin film of paint to intense motions inside stars. It is a part of all atmospheric and oceanic circulations, the generation of planetary magnetic fields, and myriad engineering processes that involve heat transport. When the convective motion is turbulent, as in most examples cited above, it

---

<sup>☆</sup> From a talk given at the APCTP International Symposium on Slow Dynamical Processes in Nature, Seoul, Korea 2001. Supported by NSF grant # DMR-9529609.

\* Corresponding author.

*E-mail address:* joe@vortex.uoregon.edu (J.J. Niemela).

poses a fundamentally difficult problem involving a large number of degrees of freedom in both space and time, exhibiting strong interactions between similar as well as distant scales. A moderately surprising observation is that there appears to be a strong coupling between the large-scale circulation—or the mean “wind”—and the much smaller plumes within the boundary layers that the wind advects. In particular, the wind itself may well be due to some self-organization on the part of small-scale fluctuations in temperature (or density). Furthermore, the wind is known to exhibit irregular and sudden reversals of direction over a wide range of time scales. These features have been noted in the literature [1–3] but no systematic investigation of its properties was made until recently [4,5]. Below, we will summarize a few recent findings and provide additional data.

## 2. The basic system

The idealized system is the so-called Rayleigh–Bénard convection, which is the flow between two horizontal surfaces separated by a vertical distance  $H$ , across which a steady temperature difference  $\Delta T$  is maintained. The fluid has a kinematic viscosity  $\nu$ , a thermal diffusivity  $\kappa$ , and an isobaric coefficient of thermal expansion  $\alpha$ . There are various time scales in the basic problem: a heat diffusion time given by  $\tau_\vartheta = H^2/\kappa$ ; a momentum diffusion time,  $\tau_v = H^2/\nu$ ; and a buoyancy or free-fall time  $\tau_B = (H/\alpha g \Delta T)^{1/2}$ ,  $g$  being the gravitational acceleration. From these three time scales we can construct two dynamical similarity parameters that specify the problem (for now, without considering the lateral walls):

$$Ra = \frac{\tau_\vartheta \tau_v}{\tau_B^2} = \frac{\alpha \Delta T g H^3}{\nu \kappa}, \quad (1)$$

$$Pr = \frac{\tau_\vartheta}{\tau_v} = \frac{\nu}{\kappa}. \quad (2)$$

These two parameters known, respectively, as the Rayleigh and Prandtl numbers, describe the dynamical state of the flow completely, at least when the so-called Boussinesq approximation holds. This approximation is that no fluid property other than its density varies significantly with temperature. As detailed elsewhere [6], the experiments to be described are well within the Boussinesq regime. When the relative density variation across the layer is substantial, the approximation breaks down and a number of secondary effects come into play.

## 3. Apparatus and methods of measurement

Experimental details are presented in Ref. [7]; here, we note only a few important features of the apparatus and the measurement protocol. The working fluid is cryogenic helium gas nominally held near a temperature of 5 K. The mean pressure is varied to obtain a large range of  $Ra$  and extremely high values of it. The heated solid surfaces are annealed copper plates which are 50 cm apart vertically. In the present experiments, the fluid is confined by cylindrical lateral walls of diameter  $D$ . The aspect ratio, which

is the ratio  $D/H$ , is unity. The cylindrical walls are made of thin stainless steel, which is a poor conductor at these temperatures.

We monitor the applied heat current, the resulting averaged steady-state temperature at the two surfaces, as well as the interior fluctuations in temperature; the latter are measured by small semiconductor resistance thermometers immersed in the fluid at various locations of the cell. To measure the large-scale circulation, two of these sensors (cubes of doped germanium of side  $250\ \mu\text{m}$ ) are placed about 4.4 cm away from the sidewall in the central horizontal plane of the fluid layer and separated vertically from each other a distance of 1.27 cm. Each sensor measures fluctuations in temperature independently. Knowing the distance between the sensors, and the delay time that maximizes the correlation of their signals, we can deduce the magnitude and direction (the delay time can be of either sign) of the large-scale flow, or the thermal wind [2]. As noted earlier, the temporal and spatial dynamics of this wind are the subject of interest here.

#### 4. A simple model for turbulent convection

To put things in context, it is helpful to model turbulent convection in the spirit of the ideas developed in the early 1960s by Howard [8]. We ignore the effects of the lateral walls for the moment. For sufficiently high  $Ra$ , the strong mixing that occurs within the cell renders the time-averaged temperature in the bulk of the flow more or less uniform. Thus, the temperature gradient occurs mainly across the diffusive boundary layers attached to the top and bottom surfaces. This leads to the following process that is roughly periodic.

If we switch on the heat flux, say at time  $t = 0$ , a conductive layer begins to grow diffusively as  $\delta \propto \sqrt{\kappa t}$ . Clearly, it will not get arbitrarily large: as  $\delta$  approaches a critical size, defined such that the Rayleigh number based on it,  $g\alpha\Delta T\delta^3/\nu\kappa$  approaches its marginal stability value of about 1100 [9], the growing layer will become unstable to convection. The instability that results at these high heat fluxes will be more “violent” than one might expect under quasistatic adjustment of the control parameter. In this model, thermal “plumes”, which are masses of hot fluid (or cold fluid, if emerging from above), will be expelled from the boundary layer just as the marginal state is exceeded. This process depletes the boundary layer so it shrinks. Because a constant heat flux is being applied to the solid wall, however, the boundary layer will again grow, with the same consequences to be repeated. This describes an essentially periodic process of growth, depletion and re-growth, at a rate that is proportional to  $Ra^{2/3}$  in Howard’s model.

At asymptotically large values of  $Ra$ , it is further assumed that the plumes lose their identity within the cell through mixing, so there is no communication between the two boundary layers. The physical heat flux must then be independent of the fluid depth, with clear implications for turbulent heat transfer scaling. It is easy to show that the critical size of the boundary layer is given by  $\delta = H/2Nu$ , where the Nusselt number  $Nu$  is the “effective” thermal conductivity of the fluid normalized by its molecular value and that  $Nu \propto Ra^{1/3}$ , defining one prediction for the asymptotic heat transfer

scaling. (Because of turbulence,  $Nu$  can be very high. For example, in the experiments of Ref. [7]  $Nu$  assumes values exceeding  $10^4$ .) In Howard's model, a coherent large scale circulation does not exist. We will now discuss the modifications generated by this feature of turbulent convection.

## 5. The large-scale flow

One of the surprising experimental observations in developed turbulent convection is the organization of buoyant plumes into a large scale self-sustaining flow. Early visual observations were made by Krishnamurti and Howard [1], although it is not certain that this feature at relatively low  $Ra$  is the same as the one we now call the wind. Furthermore, the aspect ratio in Ref. [1] was relatively large compared to unity in the present experiments and those past ones to which they bear the closest resemblance. In the latter category belong the experiments at the University of Chicago (e.g., Ref. [2]) and Lyon (e.g., Ref. [3]). More recently, Qui and Tong [10] have performed additional experiments in water; while restricted to much lower  $Ra$  than the present measurements, these experiments provide quantitative data on the large-scale flow. These authors stabilized the wind by tilting of the apparatus slightly, thus making it impossible for them to observe the nonperiodic reversals in its direction.

For aspect ratio of the order unity, the wind always encompasses the entire container. It is a single roll even at high  $Ra$ , rather than two rolls with up or down flow in the center. We make this claim for two specific reasons. First, no significant large-scale velocities are measured in the cell center; second, we have measured the wind simultaneously using two pairs of vertically oriented sidewall sensors separated azimuthally by  $180^\circ$ . If there were two cells, then the velocity measured at the two sites would be parallel. In fact, the velocity is found to be anti-parallel; furthermore, when the wind changes direction on one side of the cell it does so concurrently on the other side. This is illustrated in Fig. 1 which represents a segment of a time series for temperature fluctuations measured along the sidewall at  $Ra = 4 \times 10^{11}$ . In that figure the short time scale oscillations are associated with advected plumes, and the longer time scale is associated with a reversal of the wind; i.e., the temperature oscillations change sign in relation to the mean.

The short periodic features in Fig. 1 reflect the rate  $\omega_p$  at which plumes are advected past the sensors. Measurements show that  $\omega_p = \kappa/H^2 \times 0.64Ra^{0.47}$  [4], comparable to other measurements in similar experiments at similar  $Pr$  [11]. Note that this expression differs significantly from the predictions of the model of Section 3, for which the plumes would have an ejection rate proportional to  $Ra^{2/3}$ . This discrepancy is an indication of the strong coupling between the plumes and the wind. In fact, we find that to good approximation  $\omega_p \sim V_m/4H$ , so that the plume frequency is directly related to the circulation time of the wind. This type of self-organization is discussed by Villiermaux [12] in the context in which the top and bottom boundary layers are treated as two oscillators coupled by a large-scale recirculating flow. On the other hand, in experiments where the wind is weak or nonexistent (e.g., at large  $Pr$  [13], or at moderate  $Pr$  but

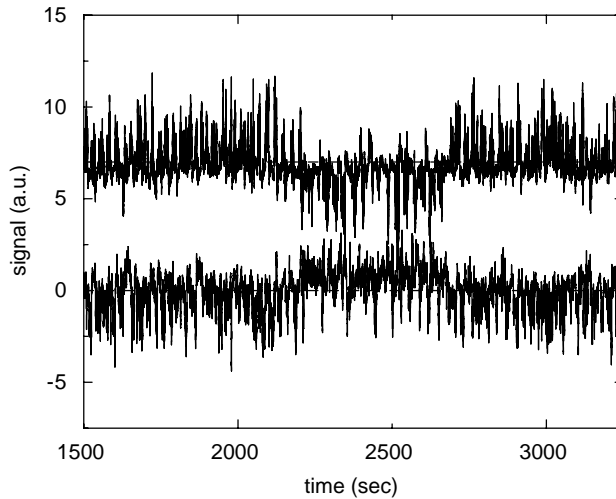


Fig. 1. Time traces of temperature from two sidewall sensors. The two sensors are located  $180^\circ$  apart in the azimuthal angle, in the central horizontal plane of the cell. The dashed lines represent the time average values. The upper trace has been shifted vertically 7 units for clarity. The two main features shown are: (1) an oscillation of the temperature, corresponding to the advection of plumes which is in opposite sense for the two sensors, and (2) a simultaneous reversal of the deviation about the mean values of the two signals.

in the absence of an upper boundary plate [14]), a periodicity consistent with that predicted in Section 3 is observed.

Fig. 2 is a segment of the wind velocity at a fixed location along the sidewall, and illustrates the “sudden” reversal of its direction. A longer time trace lasting about 5.5 days shows that these reversals are nonperiodic. By “sudden” we mean that the reversals occur on a time scale much less than one turnover time. The magnitude of the wind is the same in either direction, which would seem to imply that either the circulating roll maintains its circulation but suddenly rotates azimuthally by  $180^\circ$ , or that it is reasonably fixed in place but is occasionally stopped, and then reversed, in its direction. From the present method of observation we cannot directly distinguish between these two possibilities. It is tempting to think that because of cylindrical symmetry of the container, the first is the more likely and that the second may be too costly in terms of the energy transport. We shall consider this issue below.

## 6. Energy transport by the wind

To understand how large a perturbation is needed to reverse the wind, we have to estimate the amount of energy carried by it. We first need to estimate the size of the thermal plumes which detach from one or the other boundary layer and get advected by the mean flow. We shall assume, following Ref. [15], that the plumes have a characteristic height  $h_p$  and width  $W_p$  and occur along horizontal lines, forming thin “sheets” of buoyant fluid, as is observed experimentally at somewhat lower  $Ra$  [16].

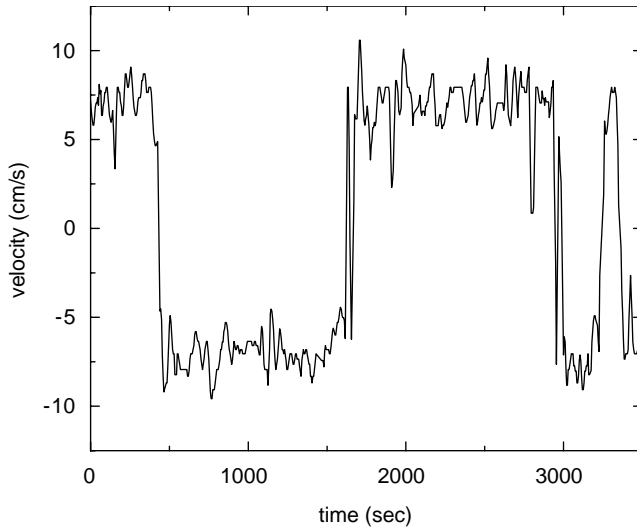


Fig. 2. A segment of the wind velocity measured from the correlation of two nearby temperature sensors, as a function of time. This segment is from a longer series extending over 5.5 days. Note that the direction reversals occur “suddenly” and that the magnitude is roughly the same in either direction.

The volume of heated fluid contained in these sheets can be estimated from a number of considerations. First,  $W_p$  must be of the order the thermal boundary layer thickness,  $\delta \simeq H/2Nu$ ;  $h_p$  is taken from Ref. [15] as being roughly  $50H Ra^{-1/3} \sim 6\delta$  at high  $Ra$ , giving a small width-to-height aspect ratio as we intuitively expect [17]. We shall take the long horizontal edge of the sheet to be of order the diameter  $D$ . This assertion is not altogether unreasonable, given that the observation of the rising (or sinking) plumes has at most a weak cosine dependence on azimuth in any section of the cell. Specifically, this is why it is not necessary to be “lucky” in the placement of probes and also why various different experiments measure roughly the same thing.

Our model of the large scale flow, then, is that the buoyant plumes, perhaps through pressure gradients associated with their detachment, initiate a horizontal wind that then advects them along the outer periphery of the cell in a coupled and self-sustaining manner. One plausible reason for the flow so initiated to be of a characteristic size  $H$  is the balance of the horizontal thermal diffusion between upward and downward jets and the viscous dissipation associated with the total path-length. Such physical considerations lead to convection rolls of the same order at the convection threshold [9]. Clearly, plumes are emitted from the entire surface of the plates, and not every plume is advected along the mean flow. In fact, the majority of the thermal emissions will be accelerated upwards into a “mixing” layer [11] and only those plumes emitted near the downstream wall will be actually advected without mixing and contribute to the sustenance of the mean wind. The extent of this region is presumably of order the viscous boundary layer  $\lambda$  set up by the wind, which can be estimated in a number of ways, but is most simply approximated for our considerations by the relation

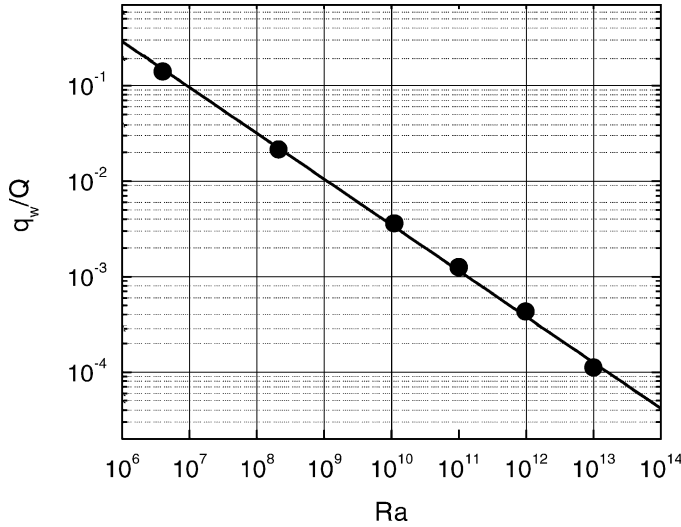


Fig. 3. The ratio of the wind power to the total applied power as a function of the Rayleigh number. The solid line represents  $219Ra^{-0.48}$ .

$\lambda \approx H/Re^{1/2}$ , at least when  $Re = V_M H/\nu$  is not very large. The typical plume spacing is not much different from  $h_p$  [15] and is larger than  $\lambda$  for all  $Ra$  in our measurements. Therefore, we assume, as above, that there is only a single line of plumes that is wholly advected about the cell.

The power  $q_w$  associated with the wind can be calculated as

$$q_w = \rho v_p C_p \Delta T \omega_p / 2\pi, \tag{3}$$

where  $C_p$  is the specific heat of the fluid of density  $\rho$ ,  $\omega_p$  is the measured rate of plume advection in our experiments, and  $v_p = 25Ra^{-1/3}H^3/Nu$  is the volume of the advected plume sheets. In Fig. 3 we show the ratio of this power to the total power  $Q$  applied to the bottom plate and transported across the depth of the fluid. The total power can be expressed as  $Nu \times Q_{cond}$ , where the heat current that would be conducted across the cell for the same gradient in temperature is, to good approximation, given by  $Q_{cond} = (\pi/4)kH\Delta T$ , neglecting the very small amount of heat conducted in parallel up the sidewall, and denoting the thermal conductivity of the fluid by  $k$ . Hence, the relative wind power can be expressed as

$$q_w/Q = 5.1\tilde{\omega}/(NuRa^{1/6})^2 \simeq 219Ra^{-0.48}, \tag{4}$$

where  $\tilde{\omega} = \omega_p H^2/\kappa$  is the dimensionless plume frequency, and we have used the experimental heat transfer correlation from our measurements,  $Nu = 0.122Ra^{0.308}$ . Thus, the wind transports a diminishing percentage of the total energy of the system as  $Ra$  is increased. This is intuitively satisfying, and can be used to help explain a number of otherwise puzzling features of the wind such as its increasing propensity to change direction at higher  $Ra$ , and the observation made in Ref. [3] that obstructing the wind

using screens had surprisingly little impact on the globally averaged heat transport across the cell.

## 7. Statistical properties of the wind

In spite of the indirect methods employed, it is possible to extract a surprising amount of information about the wind. First, in our experiments, the direction switches with equal probability for  $Ra > 10^{11}$ . Because the time scales for switching can be long (see, e.g., Fig. 2), we recorded temperature fluctuations from a pair of sensors continuously (50 Hz data rate) over the course of about  $5\frac{1}{2}$  days and at an  $Ra = 1.5 \times 10^{11}$ . Referring to Fig. 2, the zeroth order analysis consisted of examining  $T_n$ , i.e., the time at which the  $n$ th reversal occurs as a function of  $n$ . We found to a good approximation that  $T_n = \langle \tau \rangle n + \varepsilon(t)$ , where  $\langle \tau \rangle$  is the mean interval between successive zero crossings and  $\varepsilon(t)$  is the deviation of  $T_n$  about its linear trend. The deviation is found to be approximately brownian in character with a spectral density that falls off roughly as the  $-2$  power of the frequency. At this level of detail, we might conclude that there is no connection between one reversal and the next. However, if instead of  $T_n$ , we look at the interval  $\tau_r$  between the  $n$ th and  $(n+r)$ th zero crossings, i.e.,  $\tau_r = T_{n+r} - T_n$ , the probability density function for  $r=1$ ,  $p(\tau_1)$ , has a power-law roll-off as  $\tau_1^{-1}$  over more than a decade of time scales. This is a much different picture and suggests a self-similar distribution of scales at least up to some large time scale beyond which  $p(\tau_1)$  falls off exponentially as  $e^{-(\tau_1/\tau_m)}$ , indicating a Poisson-like process, with  $\tau_m \approx 400$  s. This time was connected to a diffusive relaxation time for the corner eddies in Ref. [5]. Other values of  $r$  give similar results, and different methods of analysis, including box-counting techniques to assess the coverage of the set of zero-crossings [4] also demonstrate the self-similar nature of the wind reversals.

These observations, as well as the existence of finite size scaling (see Ref. [5]) for higher order moments of the switching intervals are consistent with the concept of self-organized criticality [18–23]. There are presumably many ways in which the large scale could be generated in a system as complex as turbulent convection, but it appears from these considerations that a range of instabilities could lead to an avalanche behavior.

## 8. A plausible model

We now consider first a rather simplified dynamical model [4,5] that treats the two opposite directions of the wind as metastable states, represented by potential wells that are separated by an energy threshold barrier. Effective “noise” in the system could lead to irregular jumps between the two metastable states if the threshold were sufficiently small (or the noise level sufficiently large). The switching between two unstable states may reflect an underlying imbalance between buoyancy (which accelerates the flow of relatively warmer or colder fluid regions) and friction. Nominally, we might expect that the combined actions of buoyancy and friction would lead to a self-regulating

(steady) flow. Here it may be useful to refer to a model discussed by Welander [24] describing convection in a heated loop, which may represent the essential features of the large scale flow in confined convection to some approximation. (As an aside, it has been remarked [25,26] that this system is also governed by the Lorenz equations [27].) Welander and later experiments by Creveling et al. [28] showed that a steady flow was not always realized, and an “overshoot” could occur, say in an advected “hot” spot, which would lead to growing oscillations of the temperature field and ultimately to nonperiodic reversals of the mean flow in the loop, in analogy to the present observations.

How can we ascertain the probability  $p_R$  that a reversal will occur in our experiments? The bimodal distribution of the large-scale velocities was discussed in Refs. [7,4,5]. At low  $Ra$  there is a dominant direction which we will take to be up ( $+V_M$ ). For a sufficiently “long” velocity time series containing  $N$  cycles of the wind, the probability that the velocity will be  $+V_M$  is given by  $N_+/N$ , where  $N_+$  is the number of cycles observed having velocity  $+V_M$ . Similarly the probability that the velocity is observed to be  $-V_M$  is  $N_-/N$ , where, by our definition,  $N_- \leq N_+$ . The ratio of these probabilities is given by  $N_-/N_+$  and we should have  $N_-/N_+ = 1$  if the two directions occur with equal probability;  $N_-/N_+ = 0$  trivially when the wind is firmly fixed in direction (noting again our choice of the “dominant” direction). So a reasonable assertion is that the probability of observing a reversal is proportional to the relative number density of observed cycles in both directions over some sufficiently large number of total cycles of the wind, i.e.,  $p_R \propto N_-/N_+$ .

On the basis of our earlier assertions, we could also model  $p_R$  with a Boltzmann-like distribution:  $p_R \sim e^{-\beta E_{th}}$ , where  $E_{th}$  represents an energy threshold. In the case of closed equilibrium thermodynamic systems in contact with a reservoir at temperature  $T$ , the parameter  $\beta$  would be given by  $(k_B T)^{-1}$ , where  $k_B$  is the Boltzmann constant. As a loose analogy, we note that our *nonequilibrium* system is subject to a fixed heat current  $Q$ , or to a fixed temperature *difference* in steady-state which, in analogy to  $k_B T$  in the equilibrium case, determines the complexity of the system (see Section 2). We will then loosely interpret the inverse of  $\beta$  as some effective noise power and, to a first approximation, simply take it to be proportional to the total applied heat current, i.e.,  $\beta = (\gamma Q)^{-1}$ , where  $\gamma$  is a constant. Writing the Boltzmann factor equivalently in terms of power rather than energy, we take the threshold power to be the power associated with the sustained wind,  $q_w$  (shown in Fig. 3) so that  $p_R \sim e^{-\beta q_w}$ . Because higher values of  $Q$  are generally used to obtain higher  $Ra$ , an increase in  $p_R$  for the different  $Ra$  can be attributed to either a decrease in  $\beta = (\gamma Q)^{-1}$  or a decrease in threshold power, here represented by  $q_w$ .

In Fig. 4, we plot both the measures of the reversal probability  $p_R$  as a function of  $Ra$ . The Boltzmann form is shown as the dashed line, where we have taken  $\gamma = 0.0045$  to provide a reasonable fit to the direct measurements. For  $Ra = 10^{11}$ , where  $N_-/N_+$  becomes close to one, the power associated with the wind is only 0.1% of the total applied power, approximately equal to 1 mW. It is possible to interpret the noise in different ways. Thinking in terms of an equilibrating current from the corner region of the flow we note that  $\beta^{-1}$  can equivalently be expressed as the heat current entering the fluid laterally from the sidewall. For illustrative purposes, we may suppose that a

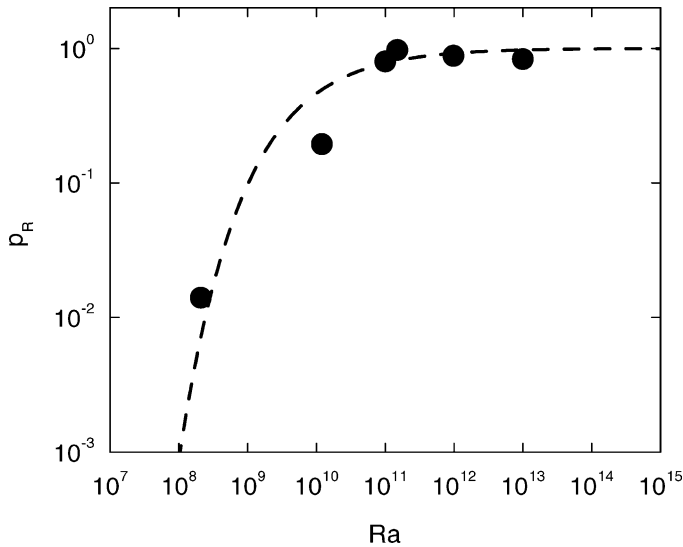


Fig. 4. The probability that the velocity undergoes reversals in direction as a function of  $Ra$ . Circles correspond to direct measurements of the bimodal probability distribution  $N_-/N_+$ . The dashed line corresponds to a Boltzmann expression  $e^{-\beta q_w}$ , with  $\beta^{-1} = 0.0045Q$ .

heat current enters the fluid through an annular cross-sectional area of circumference  $\pi D$  and height  $h$ , in the presence of a local horizontal temperature gradient in the fluid  $\Delta T/\delta$  due to the wind. Then, we can obtain  $\beta^{-1} = 0.0045Q$  by setting  $h = 0.028$  cm, which physically is approximately equal to the thermal boundary layer thickness  $\delta$  for  $Ra \sim 10^{12}$ . Naturally, other permutations of the same theme could be realized. It is worth emphasizing that even when the time series are long (5.5 days) the number of reversals,  $N$ , can still be a relatively small number (of the order 2300) vis-a-vis accurate statistical analysis, so the results here are to be viewed as essentially suggestive. The major point is that  $\beta$  is a fixed fraction of  $Q$  for all Rayleigh numbers.

## 9. Some general implications and conclusions

Because of its importance, for example in determining energy dissipation rates in stars, a scaling relation for the heat transport, valid for asymptotically large  $Ra$ , has been long sought. It is not known precisely how the mean wind might alter the heat transfer picture. A lot depends on the vigor of the wind; if the resulting boundary layers are turbulent, this may enhance the heat transfer by increasing transport through the thermal boundary layer [29]. On the other hand, as we have shown, the wind could become increasingly weaker at higher  $Ra$  and so the picture described in Section 3 may become increasingly relevant. But estimates are difficult to make and the experiments are not detailed enough at high  $Ra$  to provide definitive answers. Further, because high  $Ra$  experiments have been done with small diameter-to-height aspect ratio it is not

known exactly how the wind will orient itself in horizontally extended systems. For example, it would be interesting to know whether there will be a critical horizontal wavenumber associated with it.

In summary, we have presented a study of large scale flow in turbulent thermal convection. The “wind” of turbulence is remarkable in the sense that it seems to coordinate small-scale features of the turbulence, namely plumes, into a self-sustaining large-scale coherent motion. This flow, in turn, exhibits irregular and sudden reversals of its direction, when measured at a single point in the cell. The reversals, while seemingly random at one level of detail, reveal a self-similar structure when the methods of query are refined. The dynamical properties of the wind are conjectured to depend on a balance between buoyancy and friction, and a simple model of convection in a heated loop was considered as an analogy. Estimates of the wind power were made and compared to the total power dissipated in the cell. At low  $Ra$  the wind contains a sizable fraction of the total power in the cell, but at  $Ra \approx 10^{11}$  this drops to less than 0.1%. At this  $Ra$ , it was shown that the wind is as often in one direction as the other, which we interpret in terms of the system exceeding a threshold barrier separating two potential wells representing the metastable states  $\pm V_M$ . Taking this threshold as the energy transport by the wind over a cycle of its motion, we find such a dynamical model offers a plausible explanation for the transition to reversing flow at high  $Ra$ . Finally, it is worth remarking that there are other systems that display the behavior discussed here; in particular we note the paleomagnetic record (see, e.g., Ref. [30]) of sudden (i.e., over a span of a few thousand years) and nonperiodic reversals in the earth’s magnetic field which may persist in one direction up to times of the order 500,000 years.

## References

- [1] R. Krishnamurti, L.N. Howard, *Proc. Natl. Acad. Sci. U.S.A.* 78 (1981) 1981.
- [2] M. Sano, X.-Z. Wu, A. Libchaber, *Phys. Rev. A* 40 (1989) 6421.
- [3] S. Ciliberto, S. Cioni, C. Laroche, *Phys. Rev. E* 54 (1997) 5901.
- [4] J.J. Niemela, L. Skrbek, K.R. Sreenivasan, R.J. Donnelly, *J. Fluid Mech.* 449 (2001) 169.
- [5] K.R. Sreenivasan, A. Bershadskii, J. Niemela, *Phys. Rev. E* 65 (2002) 056306.
- [6] J.J. Niemela, K.R. Sreenivasan, R.J. Donnelly, *J. Fluid Mech.* (2002), under consideration.
- [7] J.J. Niemela, L. Skrbek, K.R. Sreenivasan, R.J. Donnelly, *Nature* 404 (2000) 837.
- [8] L. Howard, *J. Fluid Mech.* 17 (1963) 405.
- [9] S. Chandrasekhar, *Hydrodynamic and Hydromagnetic Stability*, Clarendon Press, Oxford, 1961.
- [10] X.L. Qui, P. Tong, *Phys. Rev. E* 64 (2001) 036304.
- [11] B. Castaing, G. Gunaratne, F. Heslot, L. Kadanoff, A. Libchaber, S. Thomae, X.-Z. Wu, S. Zaleski, G. Zanetti, *J. Fluid Mech.* 204 (1989) 1.
- [12] E. Villiermaux, *Phys. Rev. Lett.* 75 (1995) 4618.
- [13] N. Schaeffer, M. Manga, *Geophys. Res. Lett.* 28 (2001) 455.
- [14] E.M. Sparrow, R.B. Husar, R.J. Goldstein, *J. Fluid Mech.* 41 (1970) 793.
- [15] S.A. Theerthan, J.H. Arakeri, *J. Fluid Mech.* 373 (1998) 221.
- [16] N. Tamai, T. Asaeda, *J. Geophys. Res.* 89 (1984) 727.
- [17] D.J. Tritton, *Physical Fluid Dynamics*, 2nd Edition, Clarendon Press, 1988, Oxford.
- [18] P. Bak, *How Nature Works*, Copernicus, New York, 1996.
- [19] H.J. Jensen, *Self-Organized Criticality*, Cambridge Univ. Press, Cambridge, 1998.
- [20] R. Pastor-Satorras, A. Vespignani, *Phys. Rev. E* 61 (2000) 4854.

- [21] M. De Menech, A.L. Stella, *Phys. Rev. E* 62 (2000) R4528.
- [22] P.H. Diamond, T.S. Hahn, *Phys. Plasmas* 2 (1995) 3640.
- [23] B.A. Carreras, D. Newman, V.E. Lynch, P.H. Diamond, *Phys. Plasmas* 3 (1996) 2903.
- [24] P. Welander, *J. Fluid Mech.* 29 (1967) 17.
- [25] M. Gorman, P.J. Widmann, K.A. Robbins, *Phys. Rev. Lett.* 52 (1984) 2241.
- [26] W.V.R. Malkus, *Proceedings of the Fourth Liege Symposium on Ocean Hydrodynamics*, Mem. Soc. Roy. Sci. Leige. Collect. 8 (4) (1972) 125.
- [27] E.N. Lorenz, *J. Atmos. Sci.* 20 (1963) 130.
- [28] H.F. Creveling, J.F. De Paz, J.Y. Baladi, R.J. Schoenhals, *J. Fluid Mech.* 67 (1975) 65.
- [29] R.H. Kraichnan, *Phys. Fluids* 5 (1962) 1374.
- [30] G.A. Glatzmeier, R.C. Coe, L. Hongre, P.H. Roberts, *Nature* 401 (1999) 885.